Innovare Academic Sciences

International Journal of Pharmacy and Pharmaceutical Sciences

ISSN- 0975-1491 Vol 6, Issue 5, 2014

Original Article

IN VITRO RELEASE OF SODIUM DICLOFENAC FROM POLOXAMER 188 MODIFIED MONTMORILLONITE AS AN ORAL DRUG DELIVERY VEHICLE

MONIKA DATTA* AND MANPREET KAUR

Analytical Research laboratory, Department of Chemistry, University of Delhi, Delhi- 110007, India,
Email: monikadatta_chem@yahoo.co.in

Received: 03 Feb 2014 Revised and Accepted: 05 Mar 2014

ABSTRACT

The aim of the present work was to investigate poloxamer 188 (F-68) modified montmorillonite (Mt) clay as an oral drug delivery vehicle for in vitro release of anti-inflammatory drug- diclofenac sodium (DS). The clay (Mt) was treated with F-68 and the synthesized modified Mt, (F-68-Mt) was characterized by X-Ray diffraction (XRD) studies (which confirmed the intercalation of F-68 in the clay interlayers) and Fourier transformed infrared (FTIR) studies. The adsorption of diclofenac sodium on to the synthesized F-68-Mt was then studied as a function of pH of the aqueous drug solution, contact time and initial drug concentration. A maximum drug loading of 107.5 mg/g was obtained. The optimal drug adsorbed F-68-Mt composite was subsequently characterized by XRD studies (which confirmed the drug to be intercalated in the clay interlayers); FTIR, differential scanning calorimetric (DSC), thermogravimetric (TG), zeta potential, scanning electron microscopic (SEM) and high resolution transmission electron microscopic (HRTEM) techniques. The HRTEM image of the drug loaded sample (F-68-Mt-DS) shows the presence of drug particles less than 10 nm in dimension. The in vitro drug release studies of the intercalated drug in simulated intestinal fluid (PBS 7.4) exhibited a prolonged release as compared to the pure drug.

Keywords: Adsorption, Diclofenac sodium, *In vitro* release, Montmorillonite, Poloxamer 188.

INTRODUCTION

Clays and clay minerals play an important role in the field of health products. Their characteristic properties make them ideal for use as pharmaceutical recipients, as active ingredients or as colloidal stabilizers in the emulsion [1]. In recent years, based on their high retention capacities as well as swelling and colloidal properties, clays have been proposed as useful materials to modify drug delivery. Because of their swelling potential, clay minerals can be effectively used to delay (extended-release systems) drug release or even improve drug solubility [2].

Based on these properties, Zheng et al. [3] investigated the interaction of ibuprofen with montmorillonite clay while Park et al. [4] studied the intercalation of Donepezil, a well-known drug for Alzheimer's disease, in montmorillonite, saponite and laponite clays. Other examples of drugs effectively carried by clays include nicotine [5] and timolol [6]. Of all the clay minerals, montmorillonite (Mt) has been extensively used in pharmaceutical field. It belongs to the 2:1 smectite group of clay minerals having general formula- $M^{+}_{x+y}(Al_{2-x})(OH)_2(Si_{4-y}Al_y)O_{10}$. It has a naturally occurring layered structure having a unit thickness of 1 nm or less and it possesses high aspect ratio which makes it suitable for the synthesis of nano structured materials. It is a FDA approved excipient having rich interlayer chemistry and high potential for ion exchange. It is stable under acidic conditions and has high chemical resistance. It is associated with good hydration and swelling properties and acts as a potent detoxifier [7]. Besides it has large surface area and is known to exhibit mucoadhesive properties [2]. As a result, Mt is a common ingredient as both the excipient and active substance in pharmaceutical products [7, 8].

Poloxamers are a group of polyoxyethylene-polyoxypropylene-polyoxyethylene (PEO-PPO-PEO) block polymers widely used as a wetting and solubilising agents, tablet binders and coating [9] and more recently as surface adsorption excipients [10]. Poloxamer 188 (F-68) has 80% weight of PEO groups and this copolymer has been widely tested in numerous experimental and clinical situations [11]. The intravenous injection or infusion of poloxamer 188 has been shown to be of significant benefit in the management of sickle cell disease as well as in stroke and myocardial infarction, in which poloxamer accelerates thrombolysis, reduces re-occlusion and ameliorates re-perfusion injury. This polymer is also being evaluated for spinal cord injury and muscular dystrophy [12].

Therefore the present work was an attempt at combining the properties of both Mt and poloxamer 188 by modifying Mt with the latter and to investigate the efficiency of the resultant poloxamer 188 modified Mt as an oral drug delivery vehicle. For this anti-inflammatory drug- diclofenac sodium (DS) was chosen as the model drug. Because of its short biological half-life (1-2 hours), diclofenac sodium must be given frequently to maintain its therapeutic activity. Gastric ulcers, gastrointestinal bleeding, blood dyscrasias and anaphylaxis are potential life threatening side effects of diclofenac sodium [13]. To minimize the side effects, particularly to avoid gastric ulcers, diclofenac sodium is marketed as enteric coated and sustained release tablets. But even these formulations have shown GI toxicity in clinical studies [14]. Thus to overcome these problems, many authors have developed controlled release formulations with an intention to maintain effective diclofenac concentration for prolonged period [15, 16].

MATERIALS AND METHODS

Materials

The clay used in the present study, montmorillonite and the model drug - diclofenac sodium (DS) were obtained from Sigma Aldrich, St. Louis USA, and were used without any further purification. The triblock copolymer surfactant, poloxamer 188 (F68) was obtained from Fluka, Sigma Aldrich chemie, Germany and was used without any further purification. Double distilled water was used throughout the experimental work. The physicochemical properties of diclofenac sodium are listed in table 1.

Table 1: Physicochemical properties of diclofenac sodium

Physical properties	
Molecular formula	$C_{14}H_{10}Cl_2NNaO_2$
Chemical name	2-[(2, 6- dichlorophenyl) amino] benzene acetic acid sodium salt
Molecular weight	318.13
Absorbance maxima	277 nm
Melting point	275-277° C

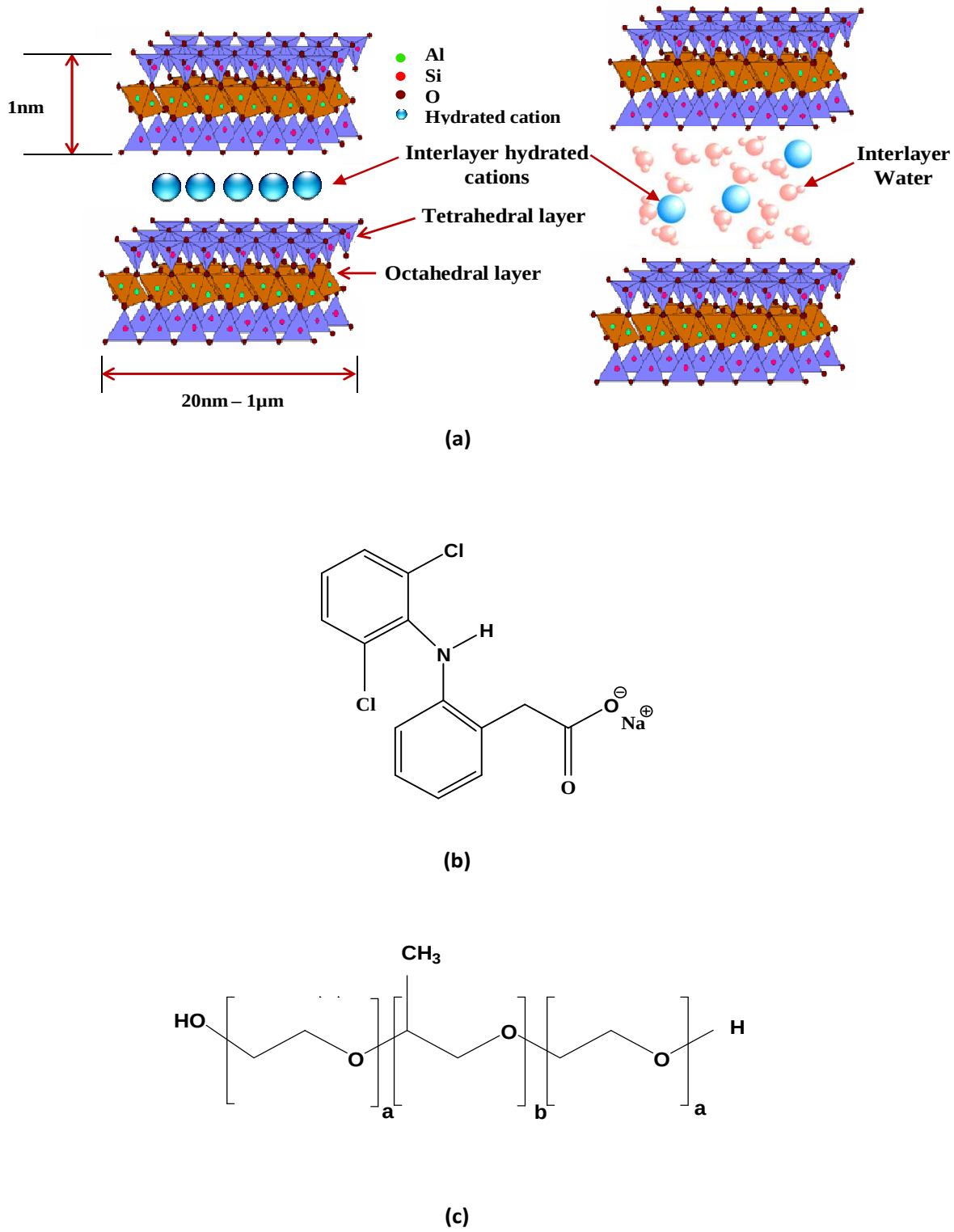

Fig. 1: Structure of (a) Montmorillonite (Mt) (b) Diclofenac sodium (c) Poloxamer 188

a = ethylene oxide, a = 80 units, b = propylene oxide, b = 27 units

Synthesis of F-68-Mt clay

The modification of Mt with F-68 was carried out by dispersing 5.0 grams of Mt and 50 mg of F-68 in 100ml of double distilled water. The contents were put on stirring on a magnetic stirrer for 2 hours after which centrifugation was done and the resultant F-68-Mt clay was subsequently lyophilized.

Characterization of synthesized F-68-Mt clay

The X-Ray diffraction (XRD) pattern of pristine Mt and F-68-Mt clay was recorded on a Philips X′ Pert-PRO PMRD system using Cu Kα radiation (n =1.54056 Å) generated at 50 kV and 100 mA. The samples were analysed in continuous scan mode at a scanning speed of 0.008°/sec operating at 2θ values between 2 to 50°. The

FTIR spectra of the samples were recorded using a Perkin-Elmer FTIR spectrophotometer using KBr matrix at room temperature over the wavenumber range 4000–400 cm^{-1} employing a total of 64 scans at a resolution of 4 cm^{-1}.

pH stability studies of aqueous drug solution

To investigate the behaviour of the aqueous drug solution at different pH values, 1000 mg/dm^3 of aqueous drug solution was maintained at pH values 1, 2, 3, 4 and 5 using 0.1/0.01N HCl standard solutions using pH 510 cyberscan pH meter (Eutech instruments). The solutions thus prepared were analysed spectrophotometrically.

Adsorption equilibrium studies of DS on F-68-Mt

Employing the batch method, the adsorption behaviour of diclofenac sodium on F-68-Mt was investigated as a function of pH of the aqueous drug solution, contact time for batch adsorption and concentration of the aqueous drug solution. Each experiment was performed using 0.05 g of adsorbent at 30 °C. To investigate the effect of pH of the aqueous drug solution on the adsorption efficiency, the aqueous drug solutions (50 mg/dm^3 concentration) in the pH range 6 to 10 were prepared. Each one of these solutions (25 ml) was treated with the adsorbent for a fixed period of 170 minutes. To study the effect of contact time on the adsorption efficiency, 25 ml of 50 mg/dm^3 of the aqueous drug solution maintained at pH 6.0 were treated with the adsorbent over a period of 20 to 190 minutes. To investigate the effect of initial drug concentration on adsorption efficiency, aqueous drug solutions having concentration in the range - 20 to 1000 mg/dm^3were prepared. Each one of these solutions (25 ml) maintained at pH 6.0 was treated with the adsorbent for a fixed time period of 170 minutes. After each set of experiment, the adsorbent was recovered by centrifugation using Sartorius 3K30 centrifuge at 20,000 rpm for 30 minutes at 20°C and the supernatant thus obtained was used for the estimation of the unadsorbed drug in the solution spectrophotometrically. The concentration of the unadsorbed drug was determined from the Beer's Lamberts plot at 277 nm with the percentage of the drug adsorbed, β and amount of drug adsorbed q_e (mg/g) being calculated using equations (1) and (2).

$$\beta = \frac{(C_i - C_e)}{C_i} \times 100 \qquad (1)$$

$$q_e = \frac{(C_i - C_e)V}{m} \qquad (2)$$

Where, C_i is the initial concentration (mg/dm^3) of the drug solution, C_e is the concentration of the drug (mg/dm^3) in the supernatant at the equilibrium stage, V is the volume of the drug solution (dm^3) and m is the mass of adsorbent employed (g).

Determination of drug encapsulation efficiency and drug content

The percentage drug content and encapsulation efficiency in the synthesized F-68-Mt drug loaded samples were calculated using equations (3) and (4) from the spectrophotometric investigations carried out at 277 nm by measuring the amount of unadsorbed drug in the aqueous solution.

$$\%\ drug\ encapsulation\ efficiency = \frac{mass\ of\ the\ drug\ loaded\ in\ the\ clay}{mass\ of\ the\ total\ drug\ added} \times 100 \qquad (3)$$

$$\%\ drug\ content = \frac{mass\ of\ the\ drug\ loaded\ in\ the\ clay}{mass of\ the\ clay\ drug\ composite\ synthesised} \times 100 \qquad (4)$$

Characterizations of the optimal F-68-Mt drug loaded composite

The X-Ray diffraction (XRD) patterns of pristine diclofenac sodium and F-68-Mt drug loaded composite (F-68-Mt-DS) were recorded using Philips X' Pert-PRO PMRD system under the same conditions as mentioned earlier. FT-IR spectra of the samples were recorded using Perkin-Elmer FT-IR spectrophotometer using KBr matrix technique under the same conditions as mentioned earlier. The differential scanning calorimetric (DSC) analyses of the samples was performed using Perkin Elmer Q200 (V23.10 build 79) system at a heating rate of 20° C/min. The samples were purged with nitrogen at a flow rate of 50.0 ml/min. Thermogravimetric analyses (TGA) of the samples was performed using Perkin-Elmer system in nitrogen atmosphere (nitrogen flow rate 20 mL/min) at a heating rate of 10 °C/min. The zeta potential measurements were performed using Malvern Zetasizer Ver. 6.01 by dispersing the samples in double distilled water. For examining the surface morphology, all the samples were sputter coated with gold and subsequently their morphology was examined using Zeiss EVO MA15 (Oxford instruments) SEM instrument equipped with energy dispersive X-Ray (EDAX) analyser. The particle size analysis was performed with high resolution transmission electron microscopic (HRTEM) technique using TECNAI G2T30 FEI Instrument. The samples were prepared by depositing the aqueous suspensions of the samples on carbon film attached to a 400 mesh Cu grid, dried overnight and subsequently the images were recorded at 300 kV.

In vitro drug release studies

The in vitro drug release behaviour of pure diclofenac sodium and the optimal clay drug composite was carried out using dialysis bag method at a constant temperature bath [6]. Buffer solution of pH 1.2 (simulated gastric fluid) was prepared by mixing 250 ml of 0.2 M HCl and 147 ml of 0.2 M KCl. Buffer solution of pH 7.4 (simulated intestinal fluid, PBS 7.4) was prepared by mixing 250 ml of 0.1 M KH_2PO_4 and 195.5 ml of 0.1 M NaOH [17]. Dialysis bags were equilibrated overnight with the dissolution medium prior to experiments. A known amount of the sample was dispersed in 5ml of the buffer solution in the dialysis bag. This dialysis bag was then immersed into the receptor compartment containing 100 ml of dissolution medium with a stirring speed of 300 rpm at 37° ± 0.5°C. The receptor compartment was closed to prevent the evaporation losses from the dissolution medium. After every one hour time interval, 5.0 ml of the sample was withdrawn and replaced with the same amount of fresh dissolution medium. The obtained 5 mL of the solution was filtrated through a membrane with a pore diameter of 0.45μm. The drug release studies were carried out for a period of 8 hours in both simulated gastric fluid (pH 1.2) and simulated intestinal fluid (PBS 7.4) separately. The concentration of the drug released was determined by UV spectrophotometer at 277 nm, and the cumulative percentage of drug released was subsequently calculated.

RESULTS AND DISCUSSION

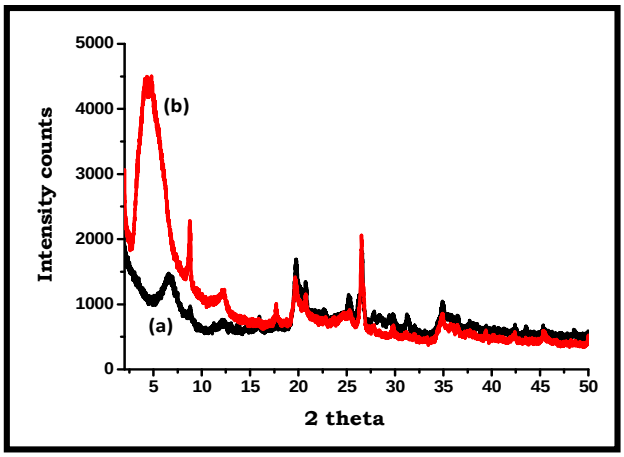

Fig. 2: XRD pattern: (a) Pristine Mt (b) F-68-Mt

Characterization of synthesized F-68-Mt clay

X-Ray diffraction (XRD) studies

To confirm the intercalation of F-68 in Mt, XRD studies were performed. The diffractogram of F-68-Mt (figure 2) indicated a shift in the peak in the lower angle region in the 001 plane w.r.t pristine Mt, from 2θ= 6.8° in the pristine Mt to 4.6° in F-68-Mt clay, resulting in an increase in the corresponding d spacing from 13.4 Å to 18.39 Å respectively. This relative increase in the d spacing confirms the intercalation of F-68 in Mt [18].

Fourier transformed infra red (FTIR) spectral studies

In the FTIR spectrum of Mt (figure 3), the band at 1049 cm^{-1} has been assigned to Si-O stretching and is the characteristic band of Mt clay [19]. The vibrational band at 1639 cm^{-1} corresponds to H-O-H bending from sorbed water. The small band at 3622 cm^{-1} corresponds to O-H stretching vibrations of the structural -OH groups [20]. The broad band ranging from 3000 to 3500 cm^{-1} in Mt has been assigned to H-O-H stretching vibrations of interlayer water which is hydrogen bonded to structural -OH groups [21]. The vibrational bands at 524 cm^{-1} and 464 cm^{-1} are strong bending vibrations corresponding to Al-O-Si and Si-O-Si respectively [22]. In the FTIR spectrum of F-68-Mt, the bands at 2925 cm^{-1} and 2876 cm^{-1} have been assigned to the C-H stretching vibrations from the methylene groups in F-68 [23]. The vibrational band at 1352 cm^{-1} corresponds to the in plane O-H bend and has been shifted to higher wave number relative to pure F-68 in which the band appears at 1344 cm^{-1}. The vibrational band at 1455cm^{-1} corresponds to the methylene bending vibrations [24].

The presence of these bands in the F-68-Mt spectrum suggests the presence of F-68 in Mt. Also, the relative decrease in the intensity of the vibrational bands at 3434 cm^{-1} and 1633 cm^{-1} in F-68-Mt in comparison to Mt indicates a decrease in the water content because of the displacement of the water molecules by F-68 which also suggests the presence of F-68 in Mt. Hence, a sharp and more intense vibrational band appears at 3624 cm^{-1} in F-68-Mt in comparison to the corresponding band at 3622 cm^{-1} in pristine Mt because of the decrease in the extent of hydrogen bonding between the interlayer water and structural -OH groups in clay.

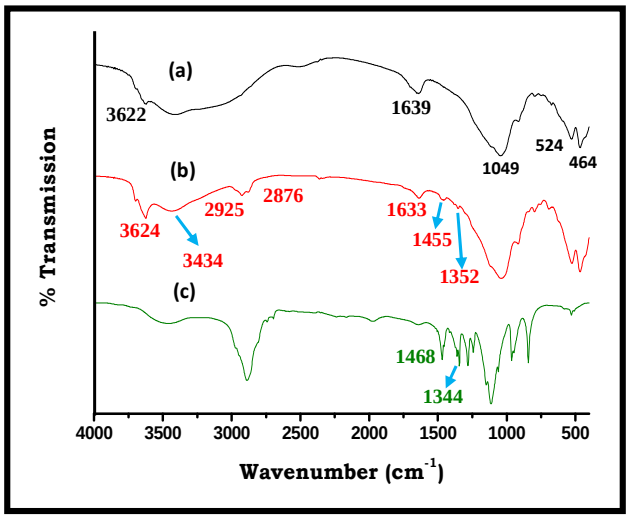

Fig. 3: FTIR spectra: (a) Pristine Mt (b) F-68-Mt (c) Pristine F-68

pH stability studies of aqueous drug solution

Since DS is a weak organic acid with pKa = 4.0 value, thus it is expected to be sparingly soluble in aqueous solutions below pH 5.0 [25, 26]. Thus the pH stability studies of aqueous drug solution were performed to observe the relative extent of precipitation of the drug below pH 5.0. The pH of the original aqueous drug solution was found to be 6.7. From the UV-VIS spectrum (figure 4), it was observed that the characteristic absorption band of diclofenac sodium at 277 nm gets diminished below pH 4.0 suggesting almost complete precipitation of the drug from the aqueous solution as diclofenac acid (scheme 1) below pH 4.0.

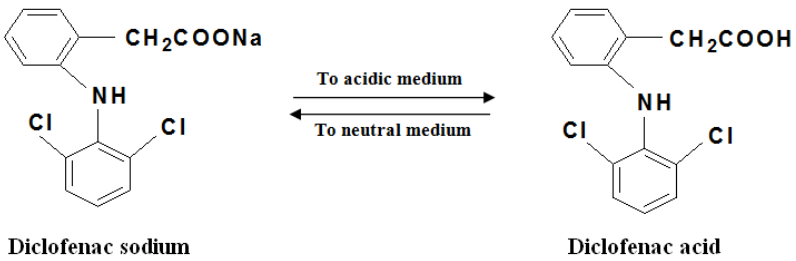

Scheme 1: pH-responsive conversion between water-soluble diclofenac sodium and water-insoluble diclofenac acid

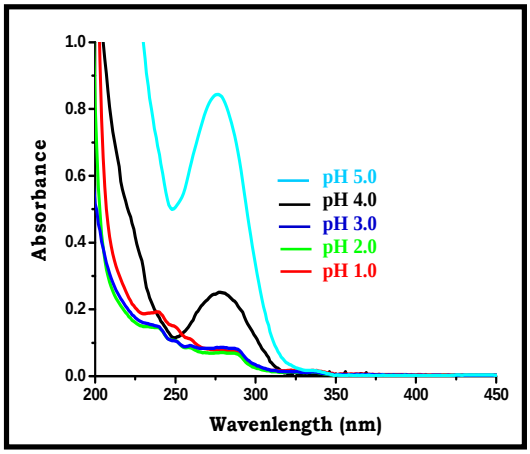

Fig. 4: Absorption spectra of drug as a function of pH of the aqueous solution

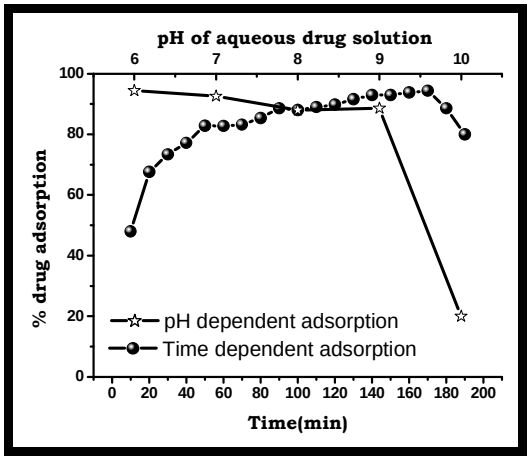

Fig. 5: Effect of pH and contact time on adsorption efficiency

Adsorption equilibrium studies of DS on F-68-Mt

Effect of pH of aqueous drug solution on adsorption efficiency

To investigate the effect of pH of the aqueous drug solution on adsorption, the pH of the aqueous drug solution was varied from 6 to 10. Because of the insolubility of the drug in the acidic medium, the above mentioned pH range was selected for the adsorption studies. It was observed that the extent of adsorption decreases with increase in the pH of the aqueous drug solution (figure 5). The maximum adsorption was found at pH 6.0 with ~95 % of the drug being adsorbed and the least at pH 10.0 showing less than 20 % adsorption.

With increase in pH, the silanol/aluminol groups on the edges of the clay get de-protonated giving rise to negatively charged surface (as shown below) which resists the adsorption of the anionic drug [27], thus showing least adsorption at pH 10.0.

$$AlOH + OH^- \longrightarrow AlO^- + H_2O$$

Effect of contact time on adsorption efficiency

An increase in adsorption was observed with an increase in the contact time for the batch adsorption studies (figure 5). The maximum adsorption was attained at 170 minutes after which the extent of adsorption started decreasing. This decrease in adsorption may arise because of the dominance of the desorption process due to the unavailability of the adsorption sites for further adsorption. The extent of adsorption is relatively faster in the beginning which can be attributed to the concentration gradient created at the start of the adsorption process between drug concentration in solution and that at the adsorbent surface.

As the drug loading on the adsorbent increases, this gradient reduces and results in a slower uptake afterwards. It was observed that with an increase in the initial drug concentration, the percentage drug adsorption decreased (figure 6). The percentage drug adsorption was higher for low initial drug concentration because of the availability of the unoccupied sorption sites on the adsorbent. However a decrease was observed with increasing drug concentration due to nearly complete coverage of the sorption sites of the adsorbents at high initial drug concentration.

Effect of initial drug concentration on adsorption efficiency

Determination of drug encapsulation efficiency and drug content

The effect of varying drug concentration on encapsulation efficiency and drug content was investigated and the results are shown in (table 2). It can be seen that the percentage encapsulation efficiency decreased with increase in the concentration of initial drug concentration. However the amount of drug adsorbed per gram of the F-68-Mt increased with increase in the initial drug concentration till 500 mg/dm^3 of drug concentration, with the clay drug composite- D13 showing maximum drug loading (107.5 mg/g). Beyond D13, a decrease in the adsorption capacity was found to occur which suggests saturation of all the adsorption sites available for the drug adsorption. Thus the clay drug composite-D13 was further characterized and subsequently studied for the in vitro drug release in simulated gastric and intestinal fluids.

Table 2: Drug encapsulation efficiency and loading in F-68-Mt clay drug composites

Sample code	Amount of F-68-Mt (mg)	Concentration of drug (mg/dm^3)	Adsorption capacity (mg/g)	% Encapsulation efficiency	% Drug content
D1	50	20	9.5	95.0	52.3
D2	50	40	19.0	94.9	51.5
D3	50	60	26.5	88.3	49.7
D4	50	80	34.1	85.3	50.2
D5	50	100	43.0	86.0	48.2
D6	50	120	50.6	84.3	43.7
D7	50	140	54.7	78.1	45.8
D8	50	160	59.0	73.8	46.9
D9	50	180	60.5	67.2	45.7
D10	50	200	66.5	66.5	42.4
D11	50	250	83.5	66.8	39.8
D12	50	350	96.2	55.0	35.6
D13	50	500	107.5	43.0	39.9
D14	50	700	99.8	28.5	38.5
D15	50	1000	90.0	18.0	40.1

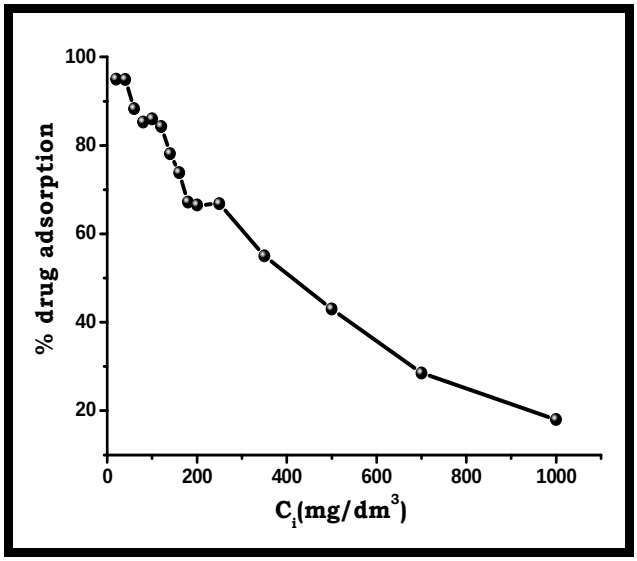

Fig. 6: Effect of initial drug concentration on adsorption efficiency

Characterizations of the optimal F-68-Mt drug loaded composite

X-Ray diffraction (XRD) studies

The XRD pattern shows a shift in the peak in the lower angle region in the 001 plane from 2θ= 4.6° in F-68-Mt to 4.0° in the drug loaded sample respectively, resulting in an increase in the corresponding d spacing from 18.39 Å to 21.4 Å respectively (figure 7). The increase in the d spacing suggests the intercalation of the drug in F-68-Mt interlayers [6]. The XRD pattern of the pure drug shows sharp peaks due to its crystalline nature. However, it is observed that no characteristic peaks of the drug are seen in the diffractogram of drug loaded sample which shows that diclofenac sodium is dispersed at the molecular level in F-68-Mt since no indication of the crystalline nature of the drug is observed [28].

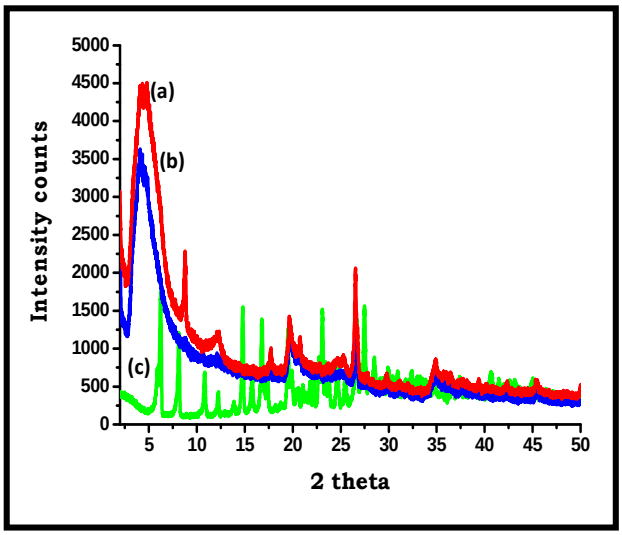

Fig. 7: XRD pattern: (a) F-68-Mt (b) F-68-Mt-DS (c) Pristine DS

Fourier transformed infrared (FTIR) spectral studies

The FTIR spectrum of the drug loaded sample (figure 8) shows the characteristic vibrational band of Mt at 1040 cm^{-1} corresponding to the Si-O stretching [19]. The sharp vibrational band at 3631 cm^{-1} corresponds to O-H stretching of surface hydroxyl group (Al, Mg)-OH in clay [20]. The broad vibrational band at 3425 cm^{-1} corresponds to the H-O-H stretching from the hydrogen bonded water [21]. The intensity of this broad band is low as compared to the corresponding band in F-68-Mt which may be because of the intercalation of the drug within the clay interlayers which further displaces the water out. This is also evident from the decrease in the intensity of the vibrational band at 1639 cm^{-1}. The band at 1465 cm^{-1} corresponds to the methylene bending vibrations from the F-68 but the position of this band is shifted from 1455 cm^{-1} in F-68-Mt to 1465 cm^{-1} in the drug loaded sample which suggests the possible non polar interaction between the F-68 intercalated in Mt and the non-polar groups in the drug.

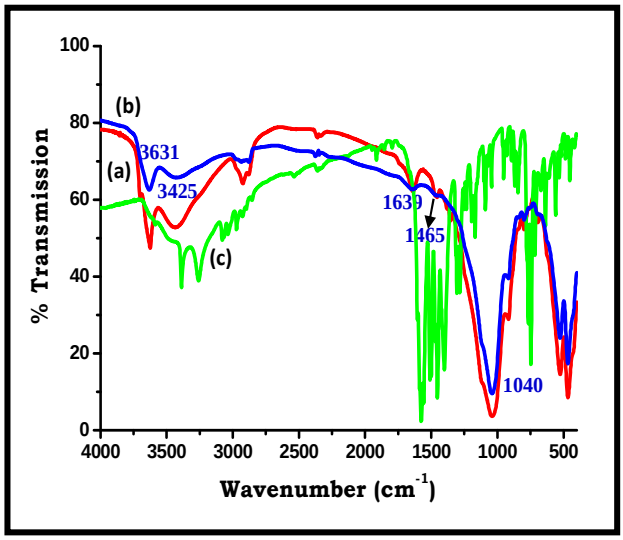

Fig. 8: FTIR spectra: (a) F-68-Mt (b) F-68-Mt-DS (c) Pristine DS

Differential scanning calorimetric (DSC) studies

To investigate the physical state of diclofenac sodium in the drug loaded sample, DSC studies were performed, (figure 9). In the DSC curve of pure drug, the melting endothermic peak appears at 292°C. This is followed by complex endothermic – exothermic phenomenon indicating decomposition of the drug

[29]. The DSC curve of F-68-Mt shows an endotherm at 70°C corresponding to the loss of surface adsorbed water followed by another at 161°C which corresponds to the loss of interlayer water. The broad endotherm c.a. 315°C corresponds to the decomposition of F-68. The endothermic peaks at 65°C and at 170°C in the DSC curve of drug loaded sample corresponds to the loss of surface adsorbed water and interlayer water respectively. The low intensity of the peak at 170°C in comparison to the corresponding peak in F-68-Mt suggests the displacement of interlayer water by the drug. Beyond this temperature, only a very broad endotherm with no well defined offset temperature is observed. The absence of melting endothermic peak of the drug in the DSC curve of the drug loaded sample suggests the uniform dispersion of the drug at the molecular level or disordered crystalline state in F-68-Mt [30].

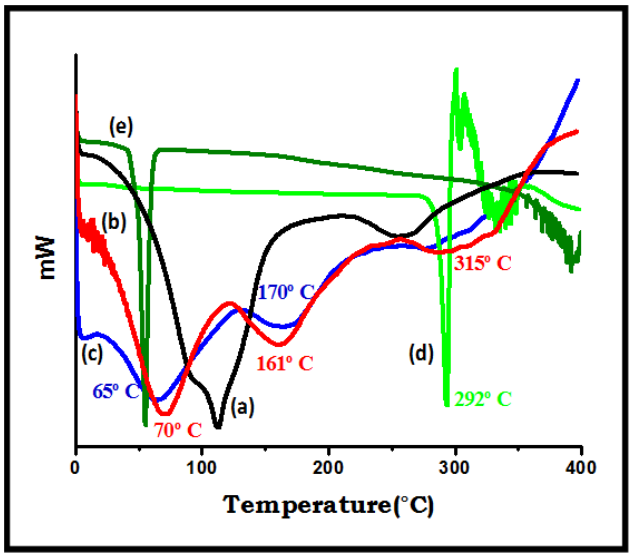

Fig. 9: DSC curves: (a) Pristine Mt (b) F-68-Mt (c) F-68-Mt-DS (d) Pristine DS (e) Pristine F-68

Thermogravimetric analysis (TGA)

The less % weight loss in the temperature range, 35° – 200° C, in case of F-68-Mt in comparison to pristine Mt indicates the displacement of the surface and interlayer water with F-68 [21] (figure 10 & table 3) and the results obtained are in agreement with the FTIR results. In case of F-68-Mt-DS, a further decrease is seen in this temperature range in comparison to F-68-Mt which suggests the further displacement of the surface and interlayer water with the drug as is evident from the FTIR results of this sample. Pristine Mt does not undergo any thermally induced changes in the 200° – 500° C temperature range [31], and F-68-Mt shows only 6.8% weight loss in this temperature range, therefore the 17.4 % weight loss seen in this range in the drug loaded sample, F-68-Mt-DS corresponds to the decomposition of the drug thus confirming the presence of the drug in F-68-Mt. It can be seen that no appreciable increase in the weight loss is seen in case of F-68-Mt in this temperature range in comparison to pristine Mt, which suggests the enhanced thermal stability of F-68 in clay interlayers, as pristine F-68 starts decomposing from 350° C onwards (see DSC curve of pristine F-68). The weight loss in the temperature range 500° – 900° C corresponds to dehydroxylation (loss of structural hydroxyl groups in Mt) [21].

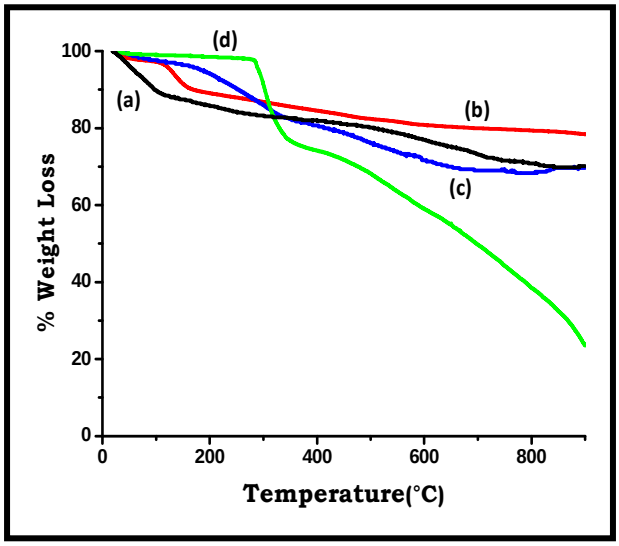

Fig. 10: TG curves: (a) Pristine Mt (b) F-68-Mt (c) F-68-Mt-DS (d) Pristine DS

Surface charge analysis using zeta potential measurement

The surface charge on F-68-Mt and the subsequent drug loaded sample, F-68-Mt-DS was found to be -35.8 mV and -39.2 mV respectively as determined by electrophoresis measurements. The negative surface charge on the F-68-Mt sample could be attributed to the presence of hydroxyl end groups present in F-68. This indicates the presence of F-68 on the surface of the clay giving it a negative charge. The surface charge on the drug loaded sample (F-68-Mt-DS) gets slightly enhanced from -35.8 mV to -39.2 mV which may be because of the presence of the presence of the negligible amount of the drug (anionic in nature) on the surface of F-68-Mt.

Scanning electron microscopic (SEM) studies with energy dispersive X-Ray (EDAX) analysis

There is a clear change in the surface morphology of F-68-Mt in comparison to pristine Mt (figure 11a) as the clay layers seem to be relatively more apart and flaky in the latter which may have been because of the intercalation of F-68 in the clay layers (as suggested by the XRD results) resulting in expansion of the basal (d) spacing. However there is not much difference in the surface morphology of the F-68-Mt after drug adsorption except the fact that the clay layers appear flakier. The EDAX data of the drug loaded sample (F-68-Mt-DS) (figure 11b) also confirms the presence of drug as indicated by the presence of elemental chlorine.

Table 3: Comparative % weight loss data

Sample code	Temperature range (ºC)	% weight loss
Pristine Mt		13.7
F-68-Mt		9.8
Pristine diclofenac sodium (DS)	35º-200º	0.8
F-68-Mt-DS		5.9
Pristine Mt		5.8
F-68-Mt	200º-500º	6.8
Pristine diclofenac sodium (DS)		30.4
F-68-Mt-DS		17.4
Pristine Mt	500º-900º	10.0
F-68-Mt		3.8
Pristine diclofenac sodium (DS)		44.0
F-68-Mt-DS		6.8

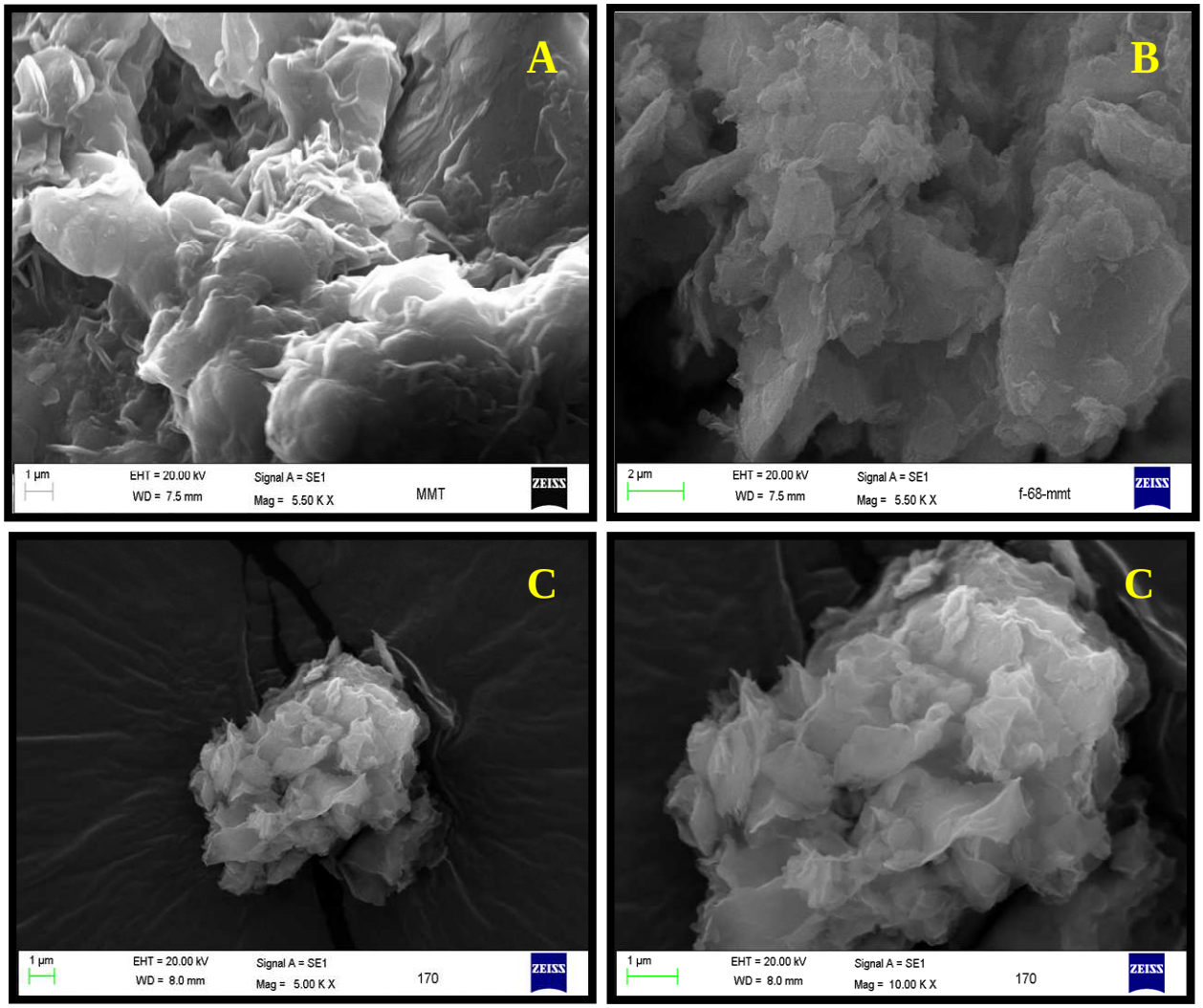

Fig. 11a: SEM images: (A) Pristine Mt (B) F-68-Mt (C) F-68-Mt-DS

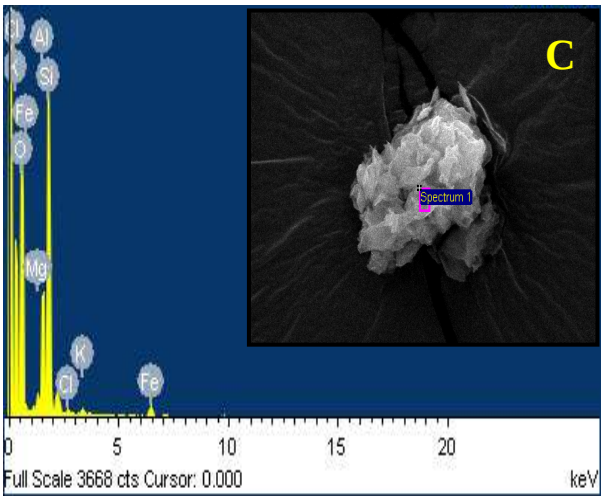

Fig. 11b: SEM-EDAX data: (C) F-68-Mt-DS

High resolution transmission electron microscopic (HRTEM) studies

The HRTEM image of the drug loaded F-68-Mt composite (F-68-Mt-DS) shows the presence of drug particles (encircled) less than 10 nm in dimension (figure 12). These particles are not visible in the HRTEM image of F-68-Mt wherein only clay layers are prominently visible in the zoomed image. The characteristic Moiré fringes can be seen in the zoomed image of the drug loaded sample indicating lamellar stacking of the drug particles in F-68-Mt [32]. The corresponding EDAX data of the drug loaded F-68-Mt composite also shows the presence of the drug as evident from the presence of nitrogen, which is not present in the elemental composition of F-68-Mt as suggested by its EDAX analysis.

In vitro drug release studies

Being a weak organic acid, diclofenac sodium shows negligible solubility in pH 1.2; therefore no drug release takes place from the drug loaded F-68-Mt composite (F-68-Mt-DS) in simulated gastric fluid (pH 1.2) (figure 13). However, 4% release was seen in the second hour and a total of 7% release was observed in 8 hours in case of pure drug.

In simulated intestinal fluid (PBS 7.4), 65% of the pristine diclofenac sodium was released in the first hour which rose to 93% in the fourth hour. As can be seen, 17% of the drug was released from the drug loaded F-68-Mt composite (F-68-Mt-DS) as compared to 65% in case of pristine diclofenac sodium in the first hour in PBS 7.4 medium. After that a prolonged release was seen and 84% of the drug release was observed in 8 hours. No burst release was observed in case of F-68-Mt drug loaded sample which shows that the drug is majorly intercalated in the modified clay. Thus F-68-Mt could successfully prolong the release of diclofenac sodium intercalated in it in comparison to the pristine diclofenac sodium in PBS 7.4 medium.

SEM-EDAX data: (C) F-68-Mt-DS

Element	Weight%	Atomic%
Mg	1.56	1.33
Al	9.90	7.59
Si	33.70	24.82
Cl	0.65	0.38
K	0.70	0.37
Fe	3.98	1.47
O	49.51	64.03
Total	100.00	

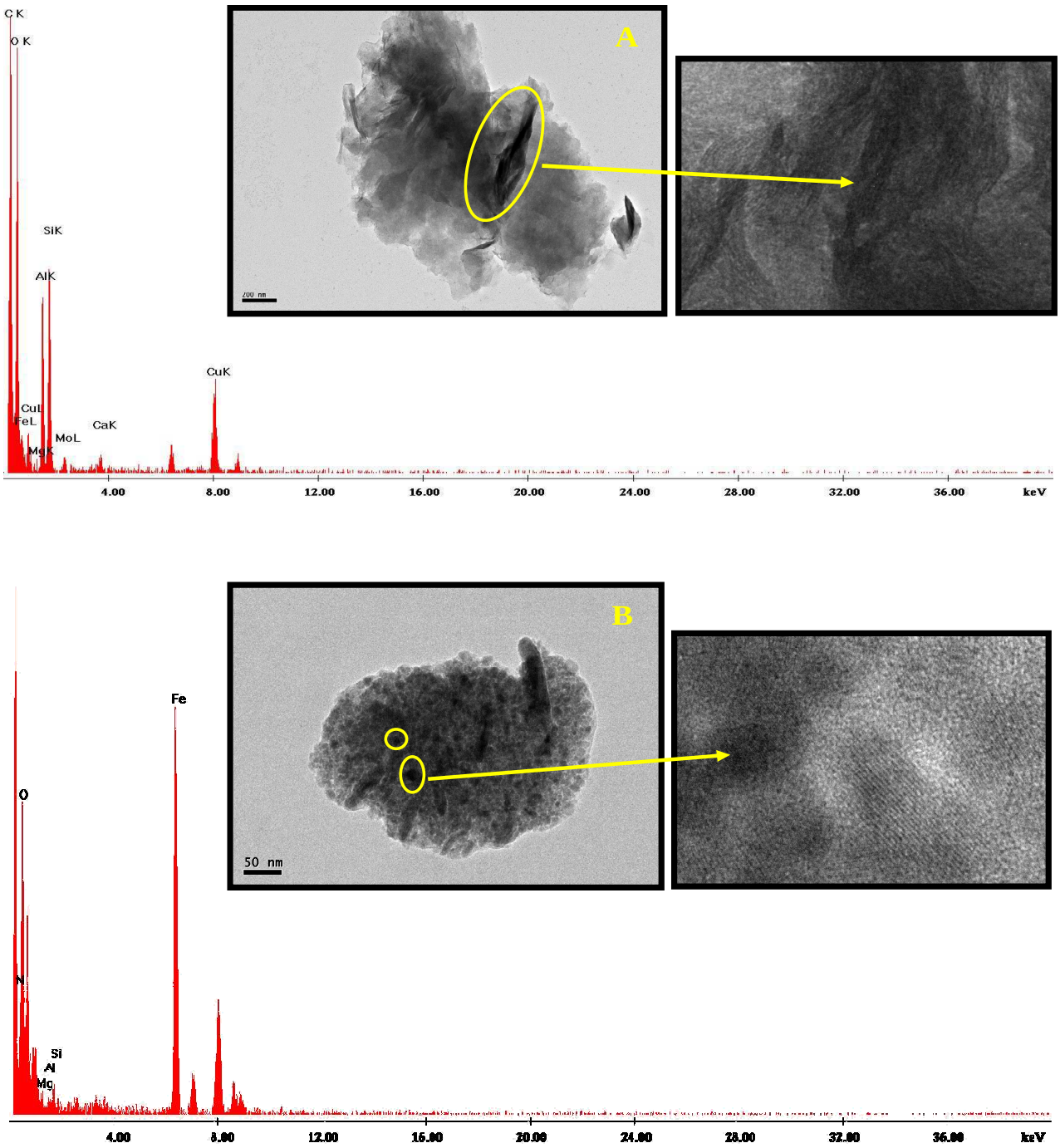

Fig. 12: HRTEM images with EDAX: (A) F-68-Mt (B) F-68-Mt-DS

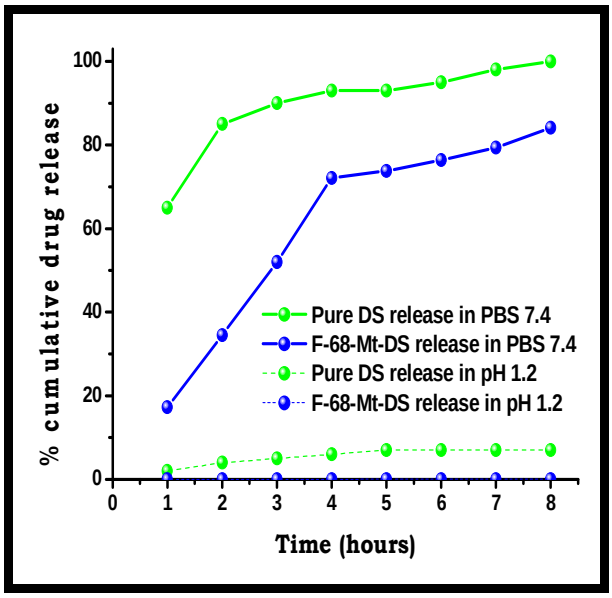

Fig.13: Drug release profile of pure drug and drug loaded sample in pH 1.2 and PBS 7.4.

CONCLUSION

The results of the present investigation suggest the intercalation of diclofenac sodium in F-68 modified Mt. A maximum drug loading of 107.5 mg/g could be achieved with the synthesized F-68-Mt clay as determined from the adsorption studies. The DSC and X-Ray diffraction studies of the drug loaded F-68-Mt composite indicate the amorphous nature of the drug entrapped in the modified clay. The FTIR spectral results indicate no strong interactions between the intercalated drug and F-68-Mt. No drug release was observed under simulated gastric conditions (pH 1.2) from the drug loaded F-68-Mt composite while the in vitro release profile in simulated intestinal fluid (PBS 7.4) revealed the ability of F-68-Mt to prolong the release of the drug as compared to that of the pristine drug. No burst release was observed and 84% of the drug was released in 8 hours. Thus on the basis of the results obtained, it can be concluded that F-68-Mt, a composite system based on clay has the potential to behave as an efficient oral drug delivery vehicle for prolonged release of diclofenac sodium.

ACKNOWLEDGEMENT

The authors are grateful to the Head, Department of Chemistry, Department of Geology and the Director of the University Science Instrumentation Centre of the University of Delhi for providing the Instrumentation facilities. We are also thankful for the financial assistance received from the University of Delhi in the form of annual research grant for carrying out the research work.

REFERENCES

1. López-Galindo A, Viseras C, Cerezo P. Compositional, technical and safety specifications of clays to be used as pharmaceutical cosmetic products. Applied Clay Science 2007; 36: 51– 63.
2. Aguzzi PC, Viseras C, Caramella C. Use of clays as drug delivery systems: Possibilities and limitations. Applied Clay Science 2007; 36: 22.
3. Zheng JP, Luan L, Wang HY, Xi LF, Yao KD. Study on ibuprofen/montmorillonite intercalation composites as drug release system. Applied Clay Science 2007; 36: 297–301.
4. Park JK, Choy YB, Oh JM, Kima JY, Hwanga SJ, Choy JH. Controlled release of donepezil intercalated in smectite clays. International Journal of Pharmaceuticals 2008; 359: 198–204.
5. Pongjanyakul T, Khunawattanakul W, Puttipipatkhachorn S. Physicochemical characterizations and release studies of nicotine–magnesium aluminum silicate complexes. Applied Clay Science 2009; 44: 242–250.
6. Joshi GV, Kevadiya BD, Patel HA, Bajaj HC, Jasra RV. Montmorillonite as a drug delivery system: Intercalation and in vitro release of timolol maleate. International Journal of Pharmaceuticals 2009; 374: 53–57.
7. Dong Y, Feng SS. Poly (D, L-lactide-co-glycolide)/montmorillonite nanoparticles for oral delivery of anticancer drugs. Biomaterials 2005; 26: 6068.
8. Takahashi T, Yamada Y, Kataoka K, Nagasaki Y. Preparation of a novel PEG–clay hybrid as a DDS material: Dispersion stability and sustained release profiles. Journal of Controlled Release 2005; 107: 408.
9. Collett JH, Popli H. Poloxamer. In: Kibbe, A.H. (Ed.), Handbook of Pharmaceutical Excipients. 3rd Edition. London: Pharmaceutical Press; 2000. p. 385–388.
10. Rouchotas C, Cassidy OE, Rowley G. Comparison of surface modification and solid dispersion techniques for drug dissolution. International Journal of Pharmaceuticals 2000; 195: 1-6.
11. Moghimi SM, Murray JC. Poloxamer-188 revisited: a potentially valuable immune modulator? Journal of the National Cancer Institute 1996; 88: 766-768.
12. Grindel JM, Jaworski T, Piraner O, Emanuele RM, Balasubramanian M. Distribution, metabolism and excretion of a novel surface-active agent, purified poloxamer 188, in rats, dogs, and humans. Journal of Pharmaceutical Sciences 2002; 91: 1936–1947.
13. Carson J, Notis WM, Orris ES. Colonic ulceration and bleeding during diclofenac therapy. The New England Journal of Medicine 1990; 323: 135–137.
14. Davies NM. Sustained release and enteric coated NSAIDs: are they really GI safe? Journal of Pharmacy and Pharmaceutical Sciences 1999; 2: 5–14.
15. Tuncay M, Calis S, Kas HS, Ercan MT, Peksoy I, Hincal AA. In vitro and in vivo evaluation of diclofenac sodium loaded albumin microspheres. Journal of Microencapsulation 2000a; 17: 145– 155.
16. Tuncay M, Calis S, Kas HS, Ercan MT, Peksoy I, Hincal AA. Diclofenac sodium incorporated PLGA (50:50) microspheres: formulation considerations and in vitro/in vivo evaluation. International Journal of Pharmaceuticals 2000b; 195: 179–188.
17. Nunes CD, Vaz PD, Fernandes AC, Ferreira P, Romao CC, Calhorda MJ. Loading and delivery of sertraline using inorganic micro and mesoporous materials. European Journal of Pharmaceutics and Biopharmacetics 2007; 66: 357-365.
18. Deng Y, Dixon JB, White GN. Intercalation and surface modification of smectite by two non-ionic surfactants. Clays and Clay Minerals 2003; 51: 150–161.
19. Nayak PS, Singh BK. Instrumental characterization of clay by XRF, XRD and FTIR. Bulletin of Material Science 2007; 30: 235–238.
20. Russel JD, Farmer VC. I.R. spectroscopic study of the dehydration of montmorillonite and saponite. Clay Minerals Bulletin 1964; 5: 443-464.
21. Kaur M, Datta M. Adsorption Characteristics of Acid Orange 10 from Aqueous Solutions onto Montmorillonite Clay. Adsorption Science and Technology 2011; 29: 301-318.
22. Farmer VC. The layer silicates. In: Farmer VC, editor. The infrared spectra of minerals. London: Mineral Soc. 1974. p. 331-364.
23. Xie Y, Li G, Yuan X, Cai Z, Rong R. Preparation and In Vitro Evaluation of Solid Dispersions of Total Flavones of Hippophae rhamnoides L. AAPS Pharmacetical Science and Technology 2009; 10: 631-640.
24. Patil SB, Shete DK, Narade SB, Surve SS, Khan ZK, Bhise SB, Pore YV. Improvement in the dissolution profile of diacerein using a surfactant-based solid dispersion technique. Drug Discovery and Therapeutics 2010; 4: 435 - 441.
25. Manca ML, Zaru M, Ennas G, Valenti D, Sinico C, Loy G, Fadda AM. Diclofenac-β-Cyclodextrin Binary Systems: Physicochemical Characterization and In Vitro Dissolution and Diffusion Studies. AAPS Pharmaceutical Science and Technology 2005; 6: 464 - 466.
26. Beck RCR, Lionzo MIZ, Costa TMH, Benvenutti EV, Ré MI, Gallas MR, Pohlmann AR, Guterres SS. Surface morphology of spray-dried nanoparticle-coated microparticles designed as an

oral drug delivery system. Brazillian Journal of Chemical Engineering 2008; 25: 389 – 398.

27. Nagy NM, Ko´nya J. The adsorption of valine on cation-exchanged montmorillonites. Applied Clay Science 2004; 25: 57– 69.
28. Konerack´a M, Muˇckova, M, Zaviˇsova V, Tomaˇsoviˇcov´a N, Kopˇcansk´y P, Timko M, Jur´ıkov´a A, Csach K, Kaveˇcansk´y V, Lancz G. Encapsulation of anticancer drug and magnetic particles in biodegradable polymer nanospheres. Journal of Physics: Condensed Matter 2008; 20: 1-7.
29. Tudja P, Khan MZI, Mestrovic E, Horvat M, Golja P. Thermal behaviour of diclofenac sodium: Decomposition and melting characteristics. Chemical and Pharmaceutical Bulletin 2001; 49: 1245-1250.
30. Yan F, Zhang C, Zheng Y, Mei L. The effect of poloxamer 188 on nanoparticle morphology, size, cancer cell uptake and cytotoxicity. Nanomedicine: Nanotechnology Biology and Medicine 2010; 6: 170-178.
31. Pastre IA, Oliveira N, Moitinho ABS, de Souza GR, Ionashiro EY, Fertonani FL.Thermal behaviour of intercalated 8- hydroxyquinoline (oxine) in montmorillonite clay. Journal of Thermal Analysis and Calorimetry 2004; 75: 661–669.
32. Lin K-J, Jeng U-S, Lin K-F. Adsorption and intercalation processes of ionic surfactants on montmorillonite associated with their ionic charge. Materials Chemistry and Physics 2011; 131: 120–126.